Atmos. Chem. Phys. Discuss., 10, 20975–21021, 2010
www.atmos-chem-phys-discuss.net/10/20975/2010/
doi:10.5194/acpd-10-20975-2010

Atmospheric Chemistry and Physics Discussions

Chemical characterization of aerosols at the summit of Mountain Tai in the middle of central east China

C. Deng[1], G. Zhuang[1], K. Huang[1], J. Li[1], R. Zhang[1], Q. Wang[1], Y. Sun[2], Z. Guo[1], and Z. Wang[3]

[1]The Center for Atmospheric Chemistry Study, Department of Environmental Science & Engineering, Fudan University, Shanghai 200433, China
[2]Department of Environmental Toxicology, University of California-Davis, Davis, California 95616, USA
[3]The Institute of Atmospheric Physics, Chinese Academy of Science, NZC/LAPC, Beijing 100029, China

Received: 13 July 2010 – Accepted: 18 August 2010 – Published: 2 September 2010

Correspondence to: G. Zhuang (gzhuang@fudan.edu.cn)

Published by Copernicus Publications on behalf of the European Geosciences Union.

Abstract

$PM_{2.5}$ and TSP samples were collected at the summit of Mountain Tai (MT) (1534 m a.s.l.) in spring 2006/2007 and summer 2006 to investigate the characteristics of aerosols over central eastern China. For comparison, aerosol samples were also collected at Tazhong, Urumqi, Tianchi in Xinjiang in northwestern China, Duolun and Yulin in northern China, and two urban sites in the megacities, Beijing and Shanghai, in spring 2007. Daily mass concentrations of TSP and $PM_{2.5}$ ranged from 39.6–276.9 μg/m^3 and 17.2–235.7 μg/m^3 respectively at the summit of MT. Averaged concentrations of $PM_{2.5}$ showed a pronounced seasonal variation with higher concentration in summer than spring. 17 water-soluble ions (SO_4^{2-}, NO_3^-, Cl^-, F^-, PO_4^{3-}, NO_2^-, CH_3COO^-, $CH_2C_2O_4^{2-}$, $C_2H_4C_2O_4^{2-}$, $HCOO^-$, MSA, $C_2O_4^{2-}$, NH_4^+, Ca^{2+}, K^+, Mg^{2+}, Na^+), and 19 elements of 176 samples from MT were measured. SO_4^{2-}, NO_3^-, and NH_4^+ were the major water-soluble species in $PM_{2.5}$, accounting for 61.5% and 73.8% of the total measured ions in spring and summer, respectively. The average ratio of $PM_{2.5}$/TSP was 0.37(2006) and 0.49(2007) in spring, while up to 0.91 in summer, suggesting that aerosol particles were primarily comprised of fine particles in summer and of considerable coarse particles in spring. Crustal elements (e.g., Ca, Mg, Al, Fe, etc.) showed higher concentration in spring than summer, while most pollution species (SO_4^{2-}, NO_3^-, K^+, NO_2^-, NH_4^+, Cl^-, organic acids, Pb, Zn, Cd, and Cr) from local/regional anthropogenic emissions and secondary formation presented higher concentration in summer. The ratio of Ca/Al and back trajectories of air mass suggested the impact of Asian dust from Gobi and deserts on the air quality in this region. The high concentration of K^+ in aerosols (4.56 μg/m^3) and its good correlation with black carbon ($r = 0.90$), oxalic acid ($r = 0.87$), and Cl^- ($r = 0.71$) were due to the severe pollution from biomass burning, which was proved to be a main source of fine particles over central eastern China in summer. Biomass burning contributed 36.71% of $PM_{2.5}$ in mass in summer. As and Pb were two of the most enriched elements, especially in spring both for TSP and $PM_{2.5}$, which revealed that the long-range transport of aerosols spread the heavy

ACPD
10, 20975–21021, 2010

pollution from coal burning everywhere over China. Anthropogenic aerosols at MT were evidently rather severe at MT, though it has been declared by UNESCO to be a World Heritage site.

1 Introduction

Aerosols have potential impact on the global atmospheric chemistry, cloud properties and precipitation development (Tegen et al., 1996; Arimoto, 2001; Rastogi and Sarin, 2005a; Rastogi and Sarin, 2006). Anthropogenic aerosols, including the primarily emissions and the secondary aerosols, are mainly in fine mode, which has much more adverse impact on climate and hydrologic cycling (Kaufman et al., 2002), visibility (Chan et al., 1999), and human health (Dockery et al., 1993).

Eastern China, including provinces of Hebei, Shandong, Jiangsu, Zhejiang, and mega-city, Shanghai, is the rapidest growth area of economy, e.g. Shandong is one of the two provinces in China, whose GDP exceeded ¥3×10^{11} RMB in 2008 (http://finance.people.com.cn/), which resulted in the increasing emissions of SO_2, NO_2, and particulate matter, and, in turn, the severe acidic precipitation (Wang et al., 2008). Mountain Tai (200×50 square kilometers) with the highest altitude (1534 m high) in central-eastern China is located in Shandong and surrounded by Jiangsu, Anhui, Henan, and Hebei provinces. Aerosols, from the summit of MT could be the representative of the regional pollution. Previous study found that CO and O_3 at the top of MT exhibited summer high and winter low, which was attributed to the seasonal changes of meteorological conditions and seasonal variations of sources (Gao et al., 2005; Wang et al., 2001a). In addition, VOCs, O_3, and CO were all higher than those observed at other rural mountainous sites (Suthawaree et al., 2010), which might be due to the strong sources surrounded. Average concentration of peroxides at MT was much lower than the measurements made at some rural mountain sites, suggesting that significant removal processes took place in this region (Ren et al., 2009). O_3 and CO play key roles in determining the oxidizing capacity of the atmosphere in the presence of sun-

ACPD
10, 20975–21021, 2010

light and they are ideal tracers for anthropogenic pollutions (Novelli et al., 1994, 1998). VOC, O_3, CO, and peroxide are all related to the formations of secondary aerosols in ambient air, which suggested that characteristics of the aerosols at MT might be different from those at other sites due to the higher levels at MT.

Mineral aerosols through long-range transport directly and indirectly affects on many properties of air mass by providing surfaces for many chemical and physical processes and serving as carriers of anthropogenic substances, which would affect on the global biogeochemical cycle and the global climate/environmental change (Guo et al., 2004; Dentener et al., 1996; Sun et al., 2004; Liu et al., 2002). Northwestern China is one of the main source areas of Asian dust, which can be transported to hundred and thousand miles away, passing through central and eastern China and even to the Pacific. The composition of mineral aerosols would subject to transform due to adsorbing gaseous species, surface reactions, and coagulation with anthropogenic aerosol on the pathway during transport.

However, previous studies on MT have been seen only on trace gases, and little on aerosols. Also, the early study on aerosols in literatures mostly focused on the samples from ground level, and limited knowledge has been acquired about the aerosols at high elevation over the world. MT is just in the downwind of outflow Asian Dust from northwestern China to the northwest Pacific. Therefore, the summit of MT is an ideal site to examine the long-range transport of Asian dust from northwestern China and to observe the mixing of dust with anthropogenic aerosol. The experiments focused on aerosol chemistry in this region were carried out in order to understand the air quality at atmospheric boundary layer over central east China. This paper characterizes the aerosols and their composition at MT, and further analyses their sources and formation processes and the relation with the long-range transport.

ACPD
10, 20975–21021, 2010

2 Experimental

2.1 Sampling

TSP and $PM_{2.5}$ aerosol samples were simultaneously collected at the meteorological observation station located at the summit of MT (36.25° N, 117.10° E) in summer 2006 (2–30 June), spring 2006 (14 March–6 May) and 2007(26 March–18 May). The sampling duration time for each sample was generally 24 h, except a few samples collected in 2007 at MT, which was 48 h. Totally 176 aerosol samples were collected on Whatman® 41 filters (Whatman Inc., Maidstone, UK) by medium-volume samplers (model: (TSP/PM_{10}/$PM_{2.5}$)–2, flow rate: 77.59 L min^{-1}). All of these filters were weighed before and after sampling with an analytical balance (Sartorius 2004MP, reading precision 10 µg) after stabilizing under constant temperature (20 °C) and humidity (40%) for over 24 h. The samples were put in polyethylene plastic bags right after sampling and reserved in a refrigerator. All the procedures were strictly quality-controlled to avoid any possible contamination of the samples. For comparison, aerosol samples were also collected at Tazhong, Urumqi, Tianchi in Xinjiang in northwestern China, Duolun and Yulin in northern China, and two urban sites in the megacities, Beijing and Shanghai, in spring 2007 (Fig. 1). The detailed analytical procedures were given elsewhere (Zhuang et al., 2001).

2.2 Chemical analysis

2.2.1 Ion analysis

One-fourth of each sample and blank filter was extracted ultrasonically by 10mL deionized water (18 MΩcm^{-1}). After passing through microporous membranes (pore size, 0.45 µm; diameter, 25 mm; made by the affiliated plant of Beijing chemical school), the filtrates were determined for pH with a pH meter (model, Orion 818). Each filtrate was stored at 4 °C in a clean tube for IC analysis. 12 anions (SO_4^{2-} , NO_3^- , Cl^-, F^-, PO_4^{3-} ,

ACPD
10, 20975–21021, 2010

NO_2^-, CH_3COO^-, $HCOO^-$, MSA, $C_2O_4^{2-}$, $CH_2C_2O_4^{2-}$, $C_2H_4C_2O_4^{2-}$) and 5 cations (NH_4^+, Ca^{2+}, K^+, Mg^{2+}, Na^+) were analyzed by Ion Chromatography (Model: Dionex 3000), which consists of a separation column (Dionex Ionpac AS11 for anion and CS12A for cation), a guard column (Dionex Ionpac AG 11 for anion and AG12A for cation), a self-regenerating suppressed conductivity detector (Dionex Ionpac ED50), and a gradient pump (Dionex Ionpac GP50). The gradient mobile phase generated by EG-3000 was used for anion detection, while the weak acid eluent (20mMMSA) for cation detection. The recovery of each ion was in the range of 80–120%. The relative standard deviation of each ion was less than 5% for reproducibility test. The limits of detection (S/N =3) were less than 0.04 mg L^{-1} for anions and 0.006 mg L^{-1} for cations. The quality assurance was routinely carried out by using Standard Reference Materials (GBW 08606) produced by National Research Center for Certified Reference Materials, China. Blank values were subtracted from sample determinations. The details were given elsewhere (Yuan et al., 2003).

2.2.2 Element analysis

Half of each sample filter and blank filter was digested at 170 °C for 4 h in high-pressure Teflon digestion vessel with 3 mL concentrated HNO_3, 1mL concentrated HCl, and 1mL concentrated HF. After cooling, the solutions were dried, and then added 0.1 mL concentrated HNO_3, and diluted to 10 mL with deionized water (resistivity of 18 MΩcm^{-1}). Total 19 elements (Al, Fe, Mn, Mg, Ti, Na, Sr, Ca, Co, Cr, Ni, Cu, Pb, Zn, Cd, V, S, As and P) were determined by Inductively Coupled Plasma Atomic Emission Spectroscopy (ICP-AES, model: ULTIMA, made by JOBIN-YVON Company, France). Black carbon (BC) was analyzed with Smokerstain Reflectometer (UK, Model, M43D). The detailed analytical procedures were given elsewhere (Zhuang et al., 2001).

ACPD
10, 20975–21021, 2010

2.3 Meteorological datafire spot map and trace gases

The meteorological data, including temperature, relative humidity (RH), dew point, wind speed, wind direction, atmospheric pressure, visibility etc., were collected from http://www.wunderground; data of SO_2, NO_2 in Shanghai and MT were collected from http://www.envir.gov.cn and http://www.tahb.gov.cn.; Fire spot data were got from MODIS Global Fire Mapping Service (http://firefly.geog.umd.edu/firemap/); O_3 and CO were detected with a commercial UV photometric analyzer (Thermo Environment Instruments Inc., Model 49) that had a detection limit of 2 ppbv and a 2-sigma (2-s) precision of 2 ppbv for a 2-min average. CO was measured with a gas filter correlation, a non-dispersive infrared analyzer (Advanced Pollution Instrumentation Inc., Model 300) with a heated catalytic scrubber for baseline determination, which was conducted every 2 h. The detection limit was 30 ppbv for a 2-min average, with a 2-s precision of about 1% for a level of 500 ppbv (2-min average). The overall uncertainty was estimated to be 10%.

3 Results and discussion

3.1 Overview of particle matters at summit of MT

3.1.1 Mass concentrations of PM and size distribution

Temporal variations of mass concentrations and the corresponding deviations of $PM_{2.5}$ and TSP at MT and other sampling sites are summarized in Fig. 2 and Tables 1–2. TSP were relatively seasonal stable (128.1 $\mu g/m^3$, 143.8 $\mu g/m^3$ in spring and 135.0 $\mu g/m^3$ in summer), while $PM_{2.5}$ has highly seasonal variation with much higher concentration in summer (123.1 $\mu g/m^3$) than spring (46.6 $\mu g/m^3$ and 70.1 $\mu g/m^3$) at MT($PM_{2.5}$ was relatively high in spring 2007 (26 March–18 May) was likely attributed to the different sampling periods compared to 2006 (14 March–6 May), which would be interpreted in

ACPD
10, 20975–21021, 2010

Sect. 3.2.1). TSP from MT was comparable with those at other sampling sites, and there was no obvious decreasing trend at a height of 1534 m as being expected. It was seen that aerosols at MT was higher than those in Shanghai but lower than those in Beijing during the study periods. Both TSP and $PM_{2.5}$ at MT were much higher than those from Tianchi, which is also located at a high elevation (1900 m). Aerosol pollutions at MT were as severe as those at ground level or even worse, e.g. $PM_{2.5}$ at MT were much higher than those at other sites at ground level in summer, such as megacities, Beijing and Shanghai. The average ratio of $PM_{2.5}$/TSP was 0.37 in spring and 0.91 in summer in 2006, indicating that fine particles dominated in summer while coarse particles in spring. The seasonal variation of fine particles should be firstly attributed to the seasonally different meteorology at MT (Table 3), which could have different impact on the air mass in boundary layer. Meteorological conditions at MT show typical seasonal variations with higher temperature, lower windy speed, lower atmospheric pressure and more solar radiation in summer than those in spring, all of which could strengthen the vertical convention of the atmosphere, so regional anthropogenic pollutants on the ground surface could easily transport upward, resulting in the increase of the height of the planetary boundary layer (PBL), even higher than the summit of MT. On the contrary, the height of the PBL layer in spring was so compressed that it used to be below the summit of MT, and the Mountain-valley breezes could not fully develop due to the weak solar radiation and the strong regional winds in ground level. Hence, the uptake of the regional pollutants to the summit was less frequent in spring than in summer, which resulted in lower concentrations of fine particles in spring. Secondly, dust storms mostly occur in spring and MT is located on the very pathway of the crustal matters from northwestern China to the northern America of the long-range transport (Arimoto et al., 1996; Zhang et al., 1997; Sun et al., 2006). Frequently windy days of high speed in spring were accompanied with high concentrations of coarse particles, even at elevation of more than 1500 m high.

ACPD
10, 20975–21021, 2010

3.1.2 Ionic and elemental composition of the particles at MT

Mass concentrations of ions in $PM_{2.5}$ and TSP at MT are listed in Table 4. Water soluble ions contributed 10.82% of TSP and 23.99% of $PM_{2.5}$ in mass concentration in spring, while 40.35% and 41.86% in summer, which revealed evidently that the secondary aerosol possessed much larger part in summer than in spring. The ratios of total ions to the total concentrations in $PM_{2.5}$ were higher than those in TSP both in summer and spring, suggesting that the pollution components prefer to be in fine mode. SO_4^{2-}, NH_4^+, NO_3^- were the major water soluble ions in both spring and summer, accounting for 61.5% in spring and 73.8% in summer of the measured ions in $PM_{2.5}$, while 69.2% and 70.8% in TSP, respectively (Table 5). Also note that higher concentration of K^+, the tracer of the biomass source, in summer and Ca^{2+}, likely more from the Asian dust source, in spring was observed, accounting for 8.4% and 22.0% of total ions in TSP, respectively.

Aerosols would exert many impacts on atmospheric processes, such as cloud formation, visibility, solar radiation, and play a major role in acidification of cloud, rain, fog, and even the formation of haze, and water-soluble ions were proved to play key roles in these processes because of their affinity with water (Tsai et al., 1999; Novakov et al., 1993; Matsumoto et al., 1997; Facchini et al., 2000). Haze days were likely to occur in stable, warm and moist air, and were characterized by the high levels of fine particles and high percentage of certain water soluble ions in the aerosols, especially for SO_4^{2-}, NO_3^-, NH_4^+. The chemical composition of aerosols at MT and Beijing in dust, haze and clear days are summarized in Table 5. The results showed that C_{IC}/C_P, $C_{(S+N+A)}/C_{IC}$, SOR and NOR at MT in summer were very similar to those in haze days in Beijing, suggesting that haze could occur frequently in summer at the summit of MT, which could be proved by the lower visibility (9.0 km) on average at MT.

Nineteen elements and black carbon (BC) in aerosols at MT are listed in Table 6, which showed clearly that crustal element (Ca, Ma, Al, Mn, Ti, Sr, and Na) were higher in spring, while pollution elements (Pb, Cr, Cd, Zn, Ni, S, BC), except for As and Cu,

ACPD
10, 20975–21021, 2010

were higher in summer. The elements could be classified into four groups according to their enrichment factors (EFs = $(X/Al)_{aerosol}/(X/Al)_{crust}$) (Fig. 3): high enriched pollution (Pb and As), medium enriched pollution (S and Zn), slightly enriched pollution (Ni, Cu and Cr) and non-enriched crustal metals (Ca, Ma, Al, Mn, Ti, Sr and Na). EFs of all crustal elements were higher in TSP and lower in $PM_{2.5}$, while pollution elements were higher in $PM_{2.5}$ and lower in TSP, respectively. EFs of As and Pb exhibited different seasonal variations with higher EF of Pb in summer and higher EF in spring of As.

3.1.3 Acidity and alkalinity of the aerosols at MT

Figure 4 shows the variations of pH of the filtrates of aerosols at MT, which revealed that pH decreased obviously from spring to summer. Mean pH values of the aqueous filtrates of aerosols at MT and other sampling sites are summed in Table 7. The aerosols at MT showed higher acidity for both $PM_{2.5}$ (pH=4.62) and TSP (pH=4.92) in summer in comparison to the weak acidity of $PM_{2.5}$ (pH=5.92) and slight alkalinity (pH=7.22) of TSP in spring. The pH of aerosols at MT in summer was the lowest among those sites at other locations, while TSP in spring showed slight alkalinity, which was similar to those from Tazhong (pH=7.39, original source of dust storm) and supper dust day in Beijing (pH=7.25, Wang et al., 2005). The higher acidity of aerosols at MT in summer was further supported by the fact that pH of rain samples in summer at MT was obviously lower than those in other seasons (Wang et al., 2006). The acidity or alkalinity of aerosols is basically restricted by the presence and the proportions of the cations and anions in aerosols. If all the cations and anions in the aerosol were measured, the ratio of equivalence concentrations of C/A (total cations/total anions) should be equal to 1. However, CO_3^{2-} and HCO_3^- were not measured in this study due to the limitation of ion chromatography, hence, the difference of the total anions and cations could be used to roughly estimate the amount of CO_3^{2-} or HCO_3^- unmeasured. C/A of aerosols in spring at MT reached 1.6, while only 1.1 in summer, suggesting that much more carbonate or bicarbonate presented in aerosols in spring. The obvious increase of SO_4^{2-}, NO_3^- and

ACPD
10, 20975–21021, 2010

organic acids and the decrease of Ca^{2+}, Mg^{2+} in aerosols at MT in summer revealed that in summer much more aerosols at MT from secondary pollution ions, which would lead to the lower pH of the filtrates of the aerosols. As a comparison, aerosols from Shanghai in summer were of less acidity and less seasonal variation (pH of 5.27 and 5.29 in $PM_{2.5}$ and 6.48 and 6.37 in TSP in spring and summer, respectively) than those at MT, which suggested that the air pollution at MT in summer was even severer than that in urban area of Shanghai.

3.2 Sources and formation mechanisms of aerosols at summit of MT

3.2.1 Influence of biomass burning

Biomass burning includes grassland, forest, and crop residue, with more than 60% attributed to crop residue burning in the world (Streets et al., 2003b). China has a large rural population whose major energy source was used to be biofuel. However, rapid economic development has increased rural access to commercial energy, and the use of biofuel is decreasing (EBCASY, 1992–2001). As a result, crop residue increasingly is being burned openly in the field after harvest. $\sim 5.182 \times 10^7$ ton crop residues (accounted for 40.0% of the total crop residues in China) were directly burnt openly in harvest every year, especially in central eastern China, including Shandong, Jiangsu, Henan, Hebei provinces, among those Shandong, where MT is located, was in number 1 with the largest amount of crop residues (1.798×10^7 t) to be burnt openly (Cao et al., 2007). Biomass burning emissions are known to have contributed a considerable amount of PM and gaseous pollutants into the atmosphere, and crop residues contribute more fine particles and gaseous than other biomaterial residues, when they are burnt (Cao et al., 2005; Zhu et al., 2005).

K^+ (water soluble potassium) is a good tracer for aerosols from biomass burning (Andreae, 1983). Source of total potassium ion (K^+_{Total}) in aerosols might be attributed to soot from biomass burning, sea salt and crustal dust. It was reasonably assumed then that total potassium (K^+_{Total}) is the sum of dust-derived potassium (K^+_{Crust}), sea-

ACPD
10, 20975–21021, 2010

salt-derived potassium (K^+_{SS}), and biosmoke potassium (K^+_{BB}), in which the concept is similar to that of Virkkula et al. (2006). It can be presented as follows: $K^+_{Total} = K^+_{Crust} + K^+_{SS} + K^+_{BB}$. Elemental Al and water soluble Na^+ is markers of crustal dust and sea salt. The following composition were assumed: Na: 31%, K:1.1%, Al:0%, and Na: 2.6%, K:2.9%, Al:7.7% in sea water and crustal dust, respectively (Wedepohl, 1995), which revealed that the ratios of K^+ were much lower than Na^+ in sea salt and Al in crustal dust. That is to say, composition of Na^+ and Al ought to be increase more than K^+ in the aerosols if the aerosols were attributed to sea salt and crustal dust. Temporal concentrations of K^+, Na^+ and Al in MT (Fig. 5) showed that K^+ in summer was significant high, and had a much more increase than Na^+ and Al, which suggested that the high concentrations of $PM_{2.5}$ in summer was mainly attributed to biomass burning rather than sea water and crustal dust.

K^+/Na^+ ratios of particles from sea salt is constant (0.037) (Chester, 1990), however, ratios of K^+/Al of crustal dust were not the same between samples from different sites due to the variable background value and the influence of the human activities. Assumed that minimum ratio of K^+/Al and Na^+/Al of 0.152 and 0.24 for $PM_{2.5}$ in the sample collected from MT on 26 April 2006, or 0.107 and 0.031 measured in the soil collected in MT served as background value of K^+ from crustal dust, then K^+_{BB} is given:

$$K^+_{BB=} K^+_{Total} - K^+_{Crust} - K^+_{SS}.$$

Where $K^+_{Crust}=0.152\times Al_{Aerosol}$, or $K^+_{Crust}=0.107\times Al_{Aerosol}$;

$$K^+_{SS} = (Na^+_{Total} - 0.240 \times Al_{Aerosol}) \times 0.037, \text{ or } K^+_{SS} = (Na^+_{Total} - 0.031 \times Al_{Aerosol}) \times 0.037$$

Na^+_{Total} is the concentration of Na^+ determined in $PM_{2.5}$ ($\mu g/m^3$) and $Al_{Aerosol}$ is elemental Al determined in $PM_{2.5}$($\mu g/m^3$). Very close concentrations of K^+_{BB} were found by the two methods (Fig. 6), and the averaged K^+_{BB} were 0.399 and 4.299 $\mu g/m^3$ in spring and summer for the former method, while 0.325 and 4.302 $\mu g/m^3$ for the later method. The high level of K^+_{BB} in summer suggested the significant biomass burning emissions,

ACPD
10, 20975–21021, 2010

which could also be confirmed by the fire spot data for the region in Fig. 7a–f. Fire spots near the site began to increase in May, and highly active fire disturbance appeared obviously in June. During 1–9 June (e), the fire spots spread mainly to the south of the site, and then extended to the northern places during 10–19 June(f), which was in the harvest season of wheat and rice from south to north over this region.

Li et al. (2007) and Cao et al. (2008) found very similar content of K^+ in $PM_{2.5}$ emitted from agriculture residues: 9.94 ± 11.8 and 9.56 ± 9.01(wt%) for wheat straw, and 11.38 ± 8.49(wt%) for rice straw. 9.56(wt%) of K^+ in $PM_{2.5}$ in this study was used to assess the contributions of $PM_{2.5}$ from open burning of agriculture residues during the sampling campaign (K^+_{BB}/0.0956 for biomass burning and Al/0.08 for crust dust) (Figs. 8–9), which revealed that fine particle from biomass burning accounted for 7.56% in spring, while 36.71% in summer, and even reached to 81.58% on the day of June 12. Burning of agriculture residues also resulted in the increase of other gaseous pollutants related to biomass burning, such as O_3, CO and VOCs (see next section).

The concentrations of K^+ at different sites are summarized in Table 8. K^+ at MT was much higher than those at other sites and showed strong seasonal variation with 4.41 μg/m^3 in summer , and 0.48 μg/m^3 in spring in $PM_{2.5}$. K^+ in $PM_{2.5}$ correlated well to the other aerosol species related to biomass burning, such as BC, $C_2O_4^{2-}$, Cl^-, etc. (Table 9), also indicated evidently that biomass burning was one of major contributor of the aerosols pollution in summer over central eastern China.

3.2.2 Secondary components, SO_4^{2-}, NO_3^-, and NH_4^+

The main secondary species (SO_4^{2-}, NO_3^-, and NH_4^+) in aerosols and their seasonal variations at different sites (MT, Urumqi, Beijing, and Shanghai) are summarized in Fig. 10. The results showed that these secondary ions in aerosols in summer at MT were more than five times of those in spring, while at Urumqi they were evidently greater in spring those that in summer, and in Shanghai and Beijing they were no big change between spring and summer.

ACPD
10, 20975–21021, 2010

Many studies confirmed that the composition and morphology of dust particles would be changed during their transport (Underwood et al., 2001; Song et al., 2001). The reaction of SO_2 on calcium-rich mineral aerosol was likely to play an important role in the downwind arid source regions (Dentener et al., 1996). Mineral aerosols reacted with SO_2 or NO_2 to form a layer of sulfate or nitrate on the mineral surfaces through the heterogeneous reactions (Yaacov et al., 1989), and soil particles would be coated by solutions contained sulfate and nitrate. The conversion of SO_2 and NO_2 to be SO_4^{2-} and NO_3^- in ambient air could be their major source in aerosols. Sulfur oxidation ratio (SOR) and nitrogen oxidation ratio (NOR) can indicate the efficiency of these transformations. If SOR is smaller than 0.10, the SO_4^{2-} could be from the primary emissions (Pierson et al., 1979; Truex et al., 1980), otherwise, SO_4^{2-} was produced through the photochemical oxidation from SO_2 (Ohta et al., 1990). Average concentrations of SO_4^{2-} and NO_3^- in TSP at MT were 4.47 μg/m^3 and 3.61 μg/m^3 in spring, 20.73 μg/m^3 and 8.82 μg/m^3 in summer respectively, while in Shanghai 2.28 μg/m^3 and 1.42 μg/m^3 in spring and 7.34 μg/m^3 and 5.50 μg/m^3, respectively, in summer 2006. During the study period, the average concentrations of SO_2 and NO_2 were 46.0 μg/m^3 and 24.0 μg/m^3 in spring, 34.0 μg/m^3 and 26.0 μg/m^3 in summer over Mountain Tai, while 51.0 μg/m^3 and 41.0 μg/m^3 in spring and 33.0 μg/m^3 and 19.0 μg/m^3 in summer in Shanghai. Though concentrations of the gases were basically in the same levels, the SOR and NOR were significantly different between the two sampling sites, especially in summer. The SOR and NOR in TSP at MT increased from 0.09 and 0.10 in spring to 0.32 and 0.26 in summer, while 0.06 and 0.10 to 0.12 and 0.16 in Shanghai at the same sampling time, suggesting that in summer at MT there were much higher transformation efficiency of SO_2 and NO_2 to be SO_4^{2-} and NO_3^-, which suggested that the secondary transformation in summer at MT was much more significant than that in ground site at urban Shanghai.

Many factors were likely attributed to the more effective conversion of SO_2 and NO_2 to be SO_4^{2-} and NO_3^- on the summit of the mountain. Firstly, for 80–90% of the global

ACPD
10, 20975–21021, 2010

sulfate was produced in the aqueous-phase, humidity plays a key role in the formation of sulfate from SO_2 (Jill et al., 2001). At the summit of MT, total cloud days were 5.4 and 7.0 in spring and summer, respectively, and monthly average foggy days could reach 26, sometimes even 30 in summer, while only 10 in spring. The relatively high humidity at the summit in summer is in favor of the formation of sulfate. Secondary, oxidation of SO_2 occurs via three potentially important pathways: oxidation by hydrogen peroxide, ozone, and auto-oxidation catalyzed by Fe (III) and Mn (II), and the former two were proved to be the dominative oxidation processes under certain conditions (Jill et al., 2001). Averaged concentration of total peroxide was significantly higher in summer (mean: 0.55 ± 0.67 ppbv) than in spring (mean: 0.17 ± 0.26 ppbv) (Ren et al., 2009). The O_3 in 2003 (Gao et al., 2005) and 2006 (Table 3) showed that O_3 was also higher in summer than that in spring. High levels of O_3 and peroxide in ambient air in summer accelerated the conversion of SO_2 and NO_2 to be SO_4^{2-} and NO_3^-. Lastly, the high effective oxidation of SO_2 at MT, might be related to the more abundance of hydrocarbon (RH) emitted by the abundant foliage (covering more than 90% of the surface of MT), as well as biomass burning emissions (Suthawaree, et al., 2010). O_3 accelerated the formation of SO_4^{2-} by directly reacting with SO_2 and generating OH radical that further to peroxide via cooperating with RH under light radiation. RH can react with OH radical to produce HO_2 and RO_2 ($OH + RH \xrightarrow{[O_2]} RO_2 + H_2O, NO + RO_2 \rightarrow RCHO + HO_2 + NO_2$) (Ariel et al., 2000), and HO_2 further react with SO_2 and NO_2. Higher CO level in summer also contributed to the oxidation of SO_2 by generating peroxide with OH radical ($OH + CO \xrightarrow{[O_2]} HO_2 + CO_2$). The reactive processes above would benefit the formation of organic acids: $HO_2 + RO_2 \rightarrow ROOH + O_2$. The high concentrations of diacids and the good correlations of diacids with SO_4^{2-} shown in Fig. 11 further suggested the formation mechanism of the high concentration of secondary aerosol in summer at MT.

NH_4^+ increased significantly from 1.48 µg/m^3 in spring to 10.4 µg/m^3 in summer. This was likely due to the pesticide sprayed in late May at MT, the large area of farming fields, and the stock-raise over MT region, which could produce much more NH_3 in

ACPD
10, 20975–21021, 2010

summer than in spring. Also, higher temperature in summer could lead to the higher emission of atmospheric NH_3 from animal's excrements (Sacoby et al., 2007).

3.2.3 Mineral dust in spring time

Concentrations of mineral elements (such as Ca, Al, and Fe) are good indicators for crustal aerosols. Figure 12 showed that how the temporal variations of these mineral elements impact on the ambient air quality around the sampling sites while the dust transported from west to east and spreading in central China in spring 2007. A strong dust storm occurred during 30 March–2 April and resulted in sharp increase of three mineral elements at all the monitoring sites, especially at Taizhong, Yulin, Duolun, MT, and Beijing. Ca/Al ratio had proved to be a good tracer for different dust origin areas (Wang et al., 2005; Sun et al., 2005), for Ca/Al showed remarkable dependence of the source regions for both dust aerosol and soil samples. Ratios of Ca/Al in this study and the reported data are shown in Table 10, suggested clearly, that western desert sources (Tazhong: 1.55 ± 0.22) are characterized by high Ca, while northern sources (Duolun: 0.45 ± 0.12) by low Ca, and the high Ca/Al (1.37 ± 0.22) at MT might be associate with an air mass originated from western or northwestern high-dust sources. The back trajectories further identified that the high mineral elements at MT in spring were mostly from the long-range transport of dust from northwestern China and passed through over the central/eastern China (Fig. 13). The facts mentioned above that the coarse particles dominated in spring ($PM_{2.5}$/TSP of 0.37) and the alkalinity (pH=7.22) of the TSP in spring further confirmed that the dust from long-range transport was the major source of the aerosols in spring at MT.

3.2.4 The pollution elements As and Pb

The pollution elements, As and Pb, were highly enriched in the aerosols with the EFs of 1541 and 679, in spring, while1470 and 1969 in summer in $PM_{2.5}$ at MT. The concentrations of As and Pb were of different seasonal variations with summer-high/spring-low

ACPD
10, 20975–21021, 2010

of Pb, while spring- high/summer-low of As. Statistic analysis (Table 11) revealed that Pb and As were high correlated to crustal elements in spring with the correlation coefficients of 0.701 for Pb to Al and 0.873 for Pb to Fe, while of 0.837 for As to Al and 0.778 for As to Fe. Furthermore, the correlation coefficient between Pb and As was as high as 0.949. These results indicated that both Pb and As were highly associated with the mineral components, which was long-range transported from northwestern China to MT in spring. Original dust from northwestern China would mix with As and Pb emitted from coal mining, widely distributing over northwestern China, and act as a carrier for As and Pb, which would gradually be enriched in the dust aerosol during its long-range transport. However, in summer the correlation coefficients of Pb to Al and Pb to Fe decreased to −0.184 and −0.194, while of As to Al and As to Fe to 0.469 and 0.456, and the correlation coefficient between Pb and As decreased to 0.494. These results indicated that in summer the sources of Pb and As were not from long-range transport, instead, they could be from those local/regional sources. It could be seen that Pb and As were both correlated well to Cr, Cu, and Zn in summer, suggesting that the sources of Pb and As could likely be from the local/reginal anthropogenic discharge in summer, and the strong convections of air mass would result in the pollutants at ground levels elevated to the summit of MT. The back trajectories shown in Fig. 14 indicated that the wind directions in summer at MT were mainly from south and east of MT, the central eastern China, where the economy was most developed with more anthropogenic pollution, which further demonstrated the local/regional sources of Pb and As in summer at MT. The local/regional anthropogenic source of Pb in summer could be much more than that in spring mainly from the long-range transport, which led to the seasonal variation of Pb with higher in the summer than spring.

4 Summary

Aerosols over central eastern China showed significantly season variation, with fine particles dominated in summer while coarse particles in spring. The summit of MT was

ACPD
10, 20975–21021, 2010

suffering from the invasion of long-range transported dust from northwestern China, the heavy local/regional anthropogenic emissions from the surrounding areas, and the severe secondary pollutions. Primary emissions of particles from biomass burning revealed to be a significant main source, and the aged air mass further deteriorated the air quality of this region. The high levels of peroxides and ozone, as well as the favourable meteorological conditions in the ambient air were in favour of the transformation of SO_2 and NO_x to sulfate and nitrate, which resulted in the even severe secondary pollution in this region. The high enrichment of As and Pb in the aerosols over MT indicated that the long-range transport of air mass spread the heavy pollution from coal burning everywhere over China.

Acknowledgements. This work was supported by the National Key Project of Basic Research of China (Grant No. 2006CB403704), and National Natural Science Foundation of China (Grant Nos. 20877020, 20977017, and 40575062). The authors would like to acknowledge Zhihua Wang of Shangdong University for providing the data of O_3 and CO.

References

Andreae, M. O.: Soot carbon and excess fine potassium: long-range transport of combustion-derived aerosols, Science, 220, 1148–1151, 1983.

Ariel, F. S. and Lamb, D.: The sensitivity of sulfer wet deposition to atmospheric oxidants, Atmos, Environ., 34, 1681–1690, 2000.

Arimoto R., Duce R. A., and Savoie D. L.: Relationships among aerosol constituents from Asia and the North Pacific during PEM-West, J. Geophys. Res. Atmos., 101(D1), 2011–2023, 1996.

Arimoto, R.: Eolian dust and Climate: Relationship to sources, tropospheric chemistry, transport and deposition, Earth Sci. Rev., 54, 29–42, 2001.

Cao, G., Zhang, X., Wang, Y., and Zheng, F.: Estimation of the emission from open burning of crop residues in China continent, Sci. Bulletin, 52(18), 1826–1831, 2007 (in Chinese).

Cao, G., Zhang, X., Gong, S., and Zheng, F.: Investigation on emission factors of particulate matter and gaseous pollutants from crop residue burning, Environ. Sci., 20, 50–55, 2008.

ACPD

10, 20975–21021, 2010

Cao, G., Zhang, X., Wang, D., and Zheng, F.: Inventory of atmospheric pollutants discharged from biomass burning in China continent, China Environ. Sci., 25(4), 389–393, 2005.
Cao, J. J., Chow, J. C., Watson, J. G., Wu, F., Han, Y. M., Jin, Z. D., Shen, Z. X., and An, Z. S.: Size-differentiated source profiles for fugitive dust in the Chinese Loess Plateau, Atmos. Environ., 42(10), 2261–2275, 2008.
Chan, Y. C., Simpson, R. W., Mctainsh, G. H., Vowles, P. D., Cohen, D. D., and Bailey, G. M.: Source apportionment of visibilty degradation problems in Brisbane (Australia) using the multiple linear regression technique, Atmos. Environ., 33, 3237–3250, 1999.
Chester, R.: Marine Geochemistry, Unwin Hyman, London, 698 pp., 1990.
Dentener, F. J., Carmichael, G. R., and Zhang, Y.: Role of mineral aerosol as a reactive surface in the global troposphere, J. Geophys. Res. Atmos., 101(D17), 22869–22889, 1996.
Dockery, D. W., Pope, A. C., Xu, X., Spengler, J. D., Ware, J. H., Fay, M. E., Ferris Jr., B. G., and Speizer, F. E.: An association between air pollution and mortality in six US cities, The New England Journal of Medicine, 1753–1759, 1993.
Facchini, M. C. S., Decesari, M., Mircea, S., Fuzzi, and Loglio, G.: Surface tension of atmospheric wet aerosol and cloud/fog droplets in relation to their organic carbon content and chemical composition, Atmos. Environ., 34, 4853–4857, 2000.
Gao, J., Wang, T., Ding, A., and Liu, C.: Observational study of ozone and carbon monoxide at the summit of mount Tai (1534m a.s.l.) in central-eastern China, Atmos. Environ., 39, 4779–4791, 2005.
Guo, J., Kenneth, A., Rahn, and Zhuang, G.: A mechanism for the increase of pollution elements in dust storms in Beijing, Atmos. Environ., 38, 855–862, 2004.
Jill, E. R., Oliver, V. R., Katharine, F. M., Christopher J., Eli, D. S., Vincent, A. D., Sonia, M. K., Liaquat, H., and Collett Jr., J.: Drop size-dependent S (IV) oxidation in chemically heterogeneous radiation fogs, Atmos. Environ., 35, 5717–5728, 2001.
Kaufman, Y. J., Tanre, D., and Boucher, O.: A satellite view of aerosols in the climate system, Nature, 419, 215–223, 2002.
Li, X., Wang, S., Duan, L., Hao, J., Li, C., Chen, Y., and Yang, L.: Particulate and Trace Gas Emissions from Open Burning of Wheat Straw and Corn Stover in China, Environ. Sci. Technol., 41 (17), 6052–6058, 2007.
Liu, C. L., Zhang, J., and Liu, S. M.: Physical and chemical characters of materials from several mineral aerosol sources in China, Environ. Sci., 23, 28–32, 2002.
Matsumnoto, K., Tanaka, H., Nagao, I., and Ishizaka, Y.: Contribution of particulate sulfate and

ACPD
10, 20975–21021, 2010

organic carbon to cloud condensation nuclei in the marine atmosphere, J. Geophys. Res. Lett., 24, 655–658, 1997.
Novakov, T. and Penner, J. E.: Large condensation of organic aerosols to cloud-condensation-nuclei concentration, Nature, 365, 823–826, 1993.
Novelli, P. C., Masarie, K. A., and Lang, P. M.: Distributions and recent changes of carbon monoxide in the lower troposphere, J. Geophys. Res., 103(D51), 19015–19033, 1998.
Novelli, P. C., Masarie, K. A., Tans, P. P., and Lang, P. M.: Recent changes in atmospheric carbon monoxide, Science, 263, 1587–1590, 1994.
Ohta, S. and Okita, T.: A chemical characterization of atmospheric aerosol in Sapporo, Atmos. Environ., 24A, 815–822, 1990.
Pierson, W. R., Brachaczek, W. W., and Mckee, D. E.: Sulfate emissions from catalyst equipped automobiles on the highway, J. Air Pollut. Control Assoc., 29, 255–257, 1979.
Rastogi, N. and Sarin M. M.: Long-term characterization of ionic species in aerosols from urban and high altitude sites in western India: Role of mineral dust and anthropogenic sources, Atmos. Environ, 39, 5541–5554, 2005a.
Rastogi, N. and Sarin, M. M.: Chemistry of aerosols over a semi-arid region: Evidence for acid neutralization by mineral dust, J. Geophys. Res. Lett., 33, L23815, doi:10.1029/2006GL027708, 2006.
Ren, Y., Ding, A., Wang, T., Shen, X., Guo, J., Zhang, J., Wang, Y., Xu, P., Wang, X., Gao, J., Jeffrey, L., and Collett, J.: Measurement of gas-phase total peroxides at the summit of Mount Tai in China, Atmos. Environ., 43, 1702–1711, 2009.
Sacoby, M. W. and Marc, L.: Examination of atmospheric ammonia levels near hog CAFOs, homes, and schools in Eastern North Carolina, Atmos. Environ., 41, 4977–4987, 2007.
Shen, Z. X., Cao, J. J., Li, X. X., Wang, Y. Q., Jie, D. M., and Zhang, X. Y.: Chemical characteristics of aerosol particles ($PM_{2.5}$) at a site of Horqin Sand-land in northeast China, Environmental Sciences-China, 18(4), 701–707, 2006.
Song, C. H. and Carmichael, G. R.: A three-dimensional modeling investigation of the evolution processes of dust and sea-salt particles in East Asia, J. Geophys. Res.-Atmos., 106(D16), 18131–18154, 2001.
Streets, D. G., Yarber, K. F., Woo, J. H., and Carmichael, G. R.: Biomass burning in Asia: Annual and seasonal estimates and atmospheric emissions, Global Biogeochem. Cy., 17(4), 1099, doi:10.1029/2003GB002040, 2003b.
Sun, Y., Zhuang, G., Wang, Y., Han, L., Guo, J., Dan, M., Zhang, W., Wang, Z., and Hao,

ACPD
10, 20975–21021, 2010

Z.: The air-borne particulate pollution in Beijing-concentration, composition, distribution and sources, Atmos. Environ., 38, 5991–6004, 2004.
Sun, Y. L., Zhuang, G. S., Wang, Z. F., Wang, Y., Zhang, W. J., Tang, A. H., Zhao, X. J., and Jia, L.: Regional characteristics of spring Asian dust and its impact on aerosol chemistry over northern China, Atmos. Chem. Phys. Discuss., 6, 12825–12864, doi:10.5194/acpd-6-12825-2006, 2006.
Sun, Y. L., Zhuang, G. S., Wang, Y., Zhao, X. J., Li, J., Wang, Z. F., and An, Z. S.: Chemical composition of dust storms in Beijing and implications for the mixing of mineral aerosol with pollution aerosol on the pathway, J. Geophys. Res., 110, D24209, doi:10.1029/2005JD006054, 2005.
Suthawaree, J., Kato, S., Okuzawa, K., Kanaya, Y., Pochanart, P., Akimoto, H., Wang, Z., and Kajii, Y.: Measurements of volatile organic compounds in the middle of Central East China during Mount Tai Experiment 2006 (MTX2006): observation of regional background and impact of biomass burning, Atmos. Chem. Phys., 10, 1269–1285, doi:10.5194/acp-10-1269-2010, 2010.
Tegen, I., Lacis, A. A., and Fung, I.: The influence of climate forcing of mineral aerosols from disturbed soils, Nature, 380(4), 419–422, 1996.
Truex, T. J., Pierson, W. R., and Mckee, D. E.: Sulfate in diesel exhaust. Environ. Sci. Technol., 14, 1118–1121, 1980.
Tsai, Y. I. and Cheng, M. T.: Visibility and aerosol chemical compositions near the coastal area in central Taiwan, Sci. Total Environ., 231, 37–51, 1999.
Underwood, G. M., Li, P., Al-Abadleh, H., and Grassian, V. H.: A Knudsen cell study of the heterogeneous reactivity of nitric acid on oxide and mineral dust particles, J. Phys. Chem. A., 105(27), 6609–6620, 2001.
Virkkula, A., Teinilä, K., Hillamo, R., Kerminen, V.-M., Saarikoski, S., Aurela, M., Viidanoja, J., Paatero, J., Koponen, I. K., and Kulmala, M.: Chemical composition of boundary layer aerosol over the Atlantic Ocean and at an Antarctic site, Atmos. Chem. Phys., 6, 3407–3421, doi:10.5194/acp-6-3407-2006, 2006.
Wang, T., Cheung, A., Vincent, T. F., Anson, M., and Li, Y. S.: Ozone and related gaseous pollutants in the boundary layer of eastern China: overview of the recent measurements at a rural site, Geophys. Res. Lett., 28(12), 2373–2376, 2001a.
Wang, Y., Zhuang, G., Sun, Y., and An, Z.: Water-soluble part of the aerosol in the dust storm season – evidence of the mixing between mineral and pollution aerosols, Atmos. Environ.,

ACPD
10, 20975–21021, 2010

39, 7020–7029, 2005.
Wang, Y., Zhuang, G., Sun Y., and An, Z.: The variation of characteristics and formation mechanisms of aerosols in dust, haze, and clear days in Beijing, Atmos. Environ., 40, 6579–6591, 2006.
Wang, Y., Zhuang, G., Zhang, X., Huang, K., Xu, C., Tang, A., Chen, J., and An, Z.: The ion chemistry, seasonal cycle, and sources of $PM_{2.5}$ and TSP aerosol in Shanghai, Atmos. Environ., 40, 2935–2952, 2006.
Wang, Y., Ge, F., Liu, X., Wang, W., Jia, H., and Wang, D.: Analysis of the ionic characteristics for wet droplets at Mountain Tai, China Environ. Sci., 26(4), 422–426, 2006 (in Chinese).
Wang, Y., Wai, K., Gao, J., Liu, X., Wang, T., and Wang, W.: The impacts of anthropogenic emissions on the precipitation chemistry at an elevated site in North-eastern China, Atmos. Environ., 42, 2959–2970, 2008.
Wedepohl, K. H.: The compositions of the continental crust, Geochim. Cosmochim. Acta, 59, 1217–1232, 1995.
Zhang, X. Y., Arimoto, R., and An, Z. S.: Dust emission from Chinese desert sources linked to variations in atmospheric circulation, J. Geophys. Res.-Atmos., 102(D23), 28041–28047, 1997.
Zhang, X. Y., Zhuang, G. Y., Zhu, G. H., Zhang, D., An, Z. S., Chen, T., and Huang, X. P.: Element tracers for Chinese source dust, Science in China (Series D), 39(5), 512–521, 1996.
Zhang, D., Zang, J., Shi, G., Iwasaka, Y., Matsuki, A., and Trochkine, D.: Mixture state of individual Asian dust particles at a coastal site of Qingdao, China, Atmos. Environ., 37(28), 3895–3901, 2003.
Zhu, B., Zhu, X., Zhang, Y., Zeng, L., and Zhang, Y.: Emission factors of $PM_{2.5}$ from crop straw burning, Research of Environmental Sciences (Chinese), 18(2), 29–33, 2005.
Zhuang, G., Guo, J., Yuan, H., and Zhao, C.: The compositions, sources, and size distribution of the dust storm from China in spring of 2000 and its impact on the global environment, Chin. Sci. Bull., 46(11), 895–900, doi:10.1007/BF02900460, 2001.
Yaacov, M. and Judith, G.: Heterogeneous reactions of minerals with sulfur and nitrogen oxides, J. Aerosol Sci., 20(3), 303–311, 1989.
Yuan, H., Wang, Y., and Zhuang, G. S.: The simultaneous determinationof organic acid, MSA with inorganic anions in aerosol and rainwater by ion chromatography, J. Inst. Anal., 6, 12–16, 2003.

ACPD
10, 20975–21021, 2010

Table 1. Mass concentrations of particle matters (μg/m^3) at the summit of MT.

		Average(μg/m^3)	Max(μg/m^3)	Min(μg/m^3)	Sample number
Spring(2006)	$PM_{2.5}$	46.6 ± 30.1	116.8	17.2	16
	TSP	128.1 ± 69.0	108.0	59.1	15
Summer(2006)	$PM_{2.5}$	123.1 ± 55.7	235.7	48.0	27
	TSP	135.0 ± 66.0	276.9	49.2	21
Spring(2007)	$PM_{2.5}$	70.1 ± 75.6	167.4	18.0	31
	TSP	143.8 ± 63.2	230.4	39.6	18

ACPD
10, 20975–21021, 2010

Table 2. Mass concentrations (μg/m^3) and size distributions of particles at the summit of MT and other sampling sites.

		Spring			Summer		
Sites	time	$PM_{2.5}$	TSP	$PM_{2.5}$/TSP	$PM_{2.5}$	TSP	$PM_{2.5}$/TSP
Shanghai	2003–2005[a]	135.0	293.0	0.46	72.0	167.0	0.43
	2006	32.0	108.0	0.30	20.0	61.2	0.33
	2007	25.3	80.7	0.31	30.5	91.0	0.34
MT	2006	46.6	128.1	0.37	123.1	135.0	**0.91**
	2007	70.1	143.8	0.49			
Urumqi	2007	81.9	232.5	0.35	45.9	172.6	0.27
Beijing	2002	212.6	1410.1	0.15	79.6	224.6	0.35
	2007	77.1	160.9	0.48			
Duolun	2007	64.1	176.2	0.36			
Tianchi	2007	24.0	57.7	0.42			
Yulin	2007	83.0	354.4	0.23			

[a] Wang et al., 2006;
[b] Wang et al., 2006.

ACPD
10, 20975–21021, 2010

Table 3. Meteorological conditions and concentrations of gases (O_3, CO, Peroxide) in ambient air at MT.

Month	Temp. (°C)	Dew Temp. (°C)	Humidity (%)	Visibility (kilometer)	Windy Speed (mph)	Concentrations (ppbv)		
						O_3	CO	Peroxide
March	2	−10	36	10	20	56	358	0.17
April	7	2	49	10	22	61	425	
June	17	10	60	9.0	16	71	516	0.55

Measurement method of peroxide: a 26-turn coil was used to strip the peroxides out of the air and into a liquid phase by water (0.42 mL/min), which was sucked through a 10-turn coil (0.42 mL/min) at which buffer (potassium hydrogen phthalate (KHP, Fisher Scientific) and tetrasodium ethylenediaminetetraacetate (Na4EDTA, Fluka Scientific)) and fluorescence (POPHA (Fluka Scientific), horseradish peroxidase (Sigma Chemical Co.), KHP, and Na4EDTA) solutions were added, then the liquid entered a pH booster cell that contained 30% ammonium hydroxide (Sigma Chemical Co.) to adjust solution pH from 6 to approximately 10. After going through a debubbler (0.42 mL/min), where the bubbles were removed, the fluorescence of the dimmer was detected using a fluorimeter (Spectrovision FD-100, Groton Technology Inc., Concord, MA) with excitation and emission wavelength of 326 nm and 400 nm, respectively.

ACPD
10, 20975–21021, 2010

Table 4. Water-soluble ions in $PM_{2.5}$ and TSP and the corresponding ratios of summer/spring at MT.

	Concentration($\mu g/m^3$) Spring		Summer		Ratio (Summer/Spring)	
	TSP	$PM_{2.5}$	TSP	$PM_{2.5}$	TSP	$PM_{2.5}$
NH_4^+	1.48	0.88	10.40	9.56	7.03	10.86
Na^+	0.68	0.56	1.36	1.28	2.00	2.29
K^+	0.72	0.48	4.56	4.41	6.33	9.19
Mg^{2+}	0.24	0.16	0.24	0.16	1.00	1.00
Ca^{2+}	3.04	1.72	2.88	1.76	0.95	1.02
F^-	0.13	0.11	0.02	0.03	0.15	0.27
Cl^-	0.83	0.65	2.18	2.30	2.63	3.54
MSA	0.02	0.01	0.22	0.54	11.00	54.00
$HCOO^-$	0.12	0.06	0.12	0.16	1.00	2.67
CH_3COO^-	0.27	0.23	1.83	1.32	6.78	5.74
$C_2O_4^{2-}$	0.15	0.10	0.37	0.48	2.47	4.80
$CH_2C_2O_4^{2-}$	0.42	0.22	0.65	0.49	1.55	2.23
$C_2H_4C_2O_4^{2-}$	0.02	0.01	0.04	0.10	2.00	10.00
NO_3^-	3.61	3.24	8.82	8.21	2.44	2.53
SO_4^{2-}	4.47	2.72	20.73	20.26	4.64	7.45
NO_2^-	0.03	0.03	0.12	0.14	4.00	4.67
PO_4^{3-}	0.01	n.a	0.01	0.02	1.00	
Total ions (C_{IC})	13.86	11.18	54.47	51.53	3.93	4.61
Total mass (C_P)	128.1	46.6	135	123.1	1.05	2.64
C_{IC}/ C_P (%)	10.82	23.99	40.35	41.86	3.73	1.74
Ca^{2+}/Total ions	21.93	15.38	5.29	3.42		
K^+/Total ions	5.19	4.29	8.37	8.56		

C_{IC}: Total mass concentrations of water- soluble ions ($\mu g/m^3$);
C_P: Mass concentrations of TSP or $PM_{2.5}$ ($\mu g/m^3$).

ACPD
10, 20975–21021, 2010

Table 5. SOR, NOR of ambient air and main water-soluble ions in $PM_{2.5}$ and TSP at MT and Beijing.

		MT		Beijing[a]		
		Spring	Summer	Haze days	Dust days	Clear days
$PM_{2.5}$/TSP		0.37	0.91	0.39	0.21	0.31
C_{IC}/C_P(%)	$PM_{2.5}$	23.99	41.86	53.20	9.30	15.2
	TSP	10.82	40.35	33.30	3.30	32.2
$C_{(S+N+A)}/C_{IC}$(%)	$PM_{2.5}$	61.50	73.80	87.10	63.70	73
	TSP	69.20	70.80	79.90	45.70	66.1
SOR	$PM_{2.5}$	0.08	0.31	0.27	0.29	0.15
	TSP	0.09	0.32	0.24	0.25	0.17
NOR	$PM_{2.5}$	0.09	0.22	0.22	0.09	0.13
	TSP	0.10	0.26	0.29	0.16	0.18

$C_{(S+N+A)}$: Aggregate mass concentrations of SO_4^{2-} , NO_3^- and NH_4^+ (μg/m^3);
C_{IC}: Total mass concentrations of water- soluble ions (μg/m^3);
C_P: Mass concentrations of TSP or $PM_{2.5}$ (μg/m^3);
SOR: Sulfur oxidation ratio, SOR=$n SO_4^{2-}/(n SO_4^{2-} + n SO_2)$;
NOR: Nitrogen oxidation ratio, NOR= $n NO_3^-/(n NO_3^- + n NO_2)$ (n refers to the molar concentration).
[a] Wang et al., 2006.

ACPD
10, 20975–21021, 2010

Table 6. Concentrations (μg/m^3) of elements in $PM_{2.5}$ and TSP and the corresponding ratios of summer/spring at MT.

Elements	Concentration(μg/m^3 or ng/m^3)				Ratio	
	Spring		Summer		(Summer/Spring)	
	TSP	$PM_{2.5}$	TSP	$PM_{2.5}$	TSP	$PM_{2.5}$
Al	3.01	1.20	2.20	1.96	0.73	1.63
Ca	3.95	1.75	2.61	1.72	0.66	0.98
Fe	2.18	0.81	1.69	0.71	0.77	0.88
Mg	1.02	0.35	0.50	0.42	0.50	1.19
Na	0.99	0.59	1.48	1.27	1.49	2.15
Zn	0.49	0.40	0.78	0.45	1.59	1.11
S	1.49	0.90	6.73	6.96	4.52	7.73
BC[a]	1.49	0.42	2.06	2.36	1.58	5.62
Ti	240.00	81.40	150.00	85.30	0.62	1.05
Sr	22.60	8.71	15.90	16.60	0.60	1.91
Mn	75.30	39.10	72.40	71.90	0.96	1.84
Cu	57.00	24.00	26.20	21.80	0.46	0.91
As	5.71	2.30	4.07	3.58	0.71	1.56
Cd	1.29	1.00	3.60	3.35	2.79	3.35
Co	1.79	1.01	3.48	2.78	1.94	2.75
Cr	23.00	22.90	98.50	85.40	4.28	3.73
Ni	7.49	7.41	22.70	19.80	3.03	2.67
Pb	42.20	15.20	76.50	72.00	1.81	4.74
P	94.60	36.60	130.00	84.60	1.37	2.31
V	5.35	BDL	BDL	BDL		

BDL: Below detection limits

BC: Black carbon

[a]Unit after BC: ng/m^3.

ACPD
10, 20975–21021, 2010

Table 7. pH of aqueous filtrates of $PM_{2.5}$ and TSP aerosols at different sampling sites.

Sites	Spring		Summer		Reference
	$PM_{2.5}$	TSP	$PM_{2.5}$	TSP	
MT	5.92	7.22	4.62	4.92	This study
Shanghai	5.27	6.48	5.29	6.37	This study
Urumqi	5.49	6.21			This study
Tianchi	5.81	6.35			This study
Tazhong	6.61	7.39			This study
Beijing					
Normal days	6.54	6.79	5.92	6.26	Wang et al., 2005
Supper dust days	7.25	7.54			Wang et al., 2005
Haze days	5.33	6.27			Wang et al., 2006

ACPD
10, 20975–21021, 2010

Table 8. Concentrations of K^+ in $PM_{2.5}$ at different sampling sites.

Sites	Year	Spring	Summer	Autumn	Winter
Shanghai	2003–2004[a]	0.73	0.46	0.39	1.79
	2005	0.53	0.29	0.97	0.70
	2006	0.57	0.32	2.39	1.30
	2007	0.30	0.50	1.11	0.94
MT	2006	0.48	**4.41**		
Urumqi	2007	0.77	0.96	2.68	3.56
Beijing	2002[b]	1.42	1.18		2.80

[a] Wang, et al., 2006;
[b] Wang et al., 2006.

ACPD
10, 20975–21021, 2010

Table 9. Correlation coefficients between K^+ and other measured species in summer at MT.

	K^+	$C_2O_4^{2-}$	BC	SO_4^{2-}	Cl^-	NO_3^-	NH_4^+
K^+	1.000						
$C_2O_4^{2-}$	0.869	1.000					
BC	0.904	0.781	1.000				
SO_4^{2-}	0.636	0.749	0.526	1.000			
Cl^-	0.708	0.640	0.742	0.481	1.000		
NO_3^-	0.813	0.903	0.767	0.802	0.753	1.000	
NH_4^+	0.636	0.749	0.526	1.000	0.481	0.802	1.000

ACPD
10, 20975–21021, 2010

Table 10. Ca/Al ratios for $PM_{2.5}$ during the dust case in 2007 and surface soil in Chinese desert regions.

Site	Type	Ca/Al	Reference
Tazhong	$PM_{2.5}$	1.55 ± 0.22	This study
Yulin, China	$PM_{2.5}$	0.52 ± 0.43	This study
Duolun	$PM_{2.5}$	0.45 ± 0.12	This study
Beijing	$PM_{2.5}$	1.37 ± 0.39	This study
MT	$PM_{2.5}$	1.37 ± 0.22	This study
Taklimakan Desert			
Western high-dust sources	Aerosol	1.99	Zhang et al. (1996)
Badain Juran desert			
Northern west high-dust sources	Aerosol	1.2	Zhang et al. (1996)
Hunshandake sandland		0.52	Zhang et al. (1996)
Tongliao, Horqin sand land	$PM_{2.5}$	0.76	Shen et al. (2006)
Loess Plateau	Aerosol	1.14	Zhang et al. (2003)
	TSP	1.22	Cao et al. (2008)

ACPD
10, 20975–21021, 2010

Table 11. Correlation coefficients among the certain species in spring and summer at MT.

Spring	SO_4^{2-}	NO_3^-	BC	Al	Fe	Ca	As	Cr	Cu	Cd	Mn	Pb	Zn	Ti	Summer
SO_4^{2-}		.802	.526	.253	.274	.249	.502	.325	.478	.613	.303	.496	.538	−.243	SO_4^{2-}
NO_3^-	.954		.767	.223	.237	.259	.415	.249	.594	.551	.286	.419	.557	−.087	NO_3^-
BC	.748	.792		−.030	−.029	−.002	.358	.090	.323	.378	.023	.476	.081	.004	BC
Al	.225	.185	−.027		.997	.986	.469	.795	.623	.691	.984	−.184	.725	.411	Al
Fe	.353	.239	−.070	.781		.982	.456	.775	.616	.677	.984	−.194	.733	.390	Fe
Ca	.057	.049	−.241	.857	.806		.529	.838	.684	.721	.992	−.139	.755	.482	Ca
As	.326	.234	−.061	.837	.778	.683		.786	.672	.812	.561	.494	.486	.274	As
Cr	.164	.111	−.185	.845	.832	.881	.863		.785	.847	.855	.148	.704	.372	Cr
Cu	.013	−.043	−.026	.284	.332	.313	.407	.484		.802	.700	.337	.825	.308	Cu
Cd	.478	.345	.111	.693	.692	.593	.806	.779	.609		.754	.527	.720	.204	Cd
Mn	.415	.295	-.004	.815	.963	.805	.764	.851	.320	.782		−.092	.770	.447	Mn
Pb	.438	.359	.086	.701	.873	.554	.949	.774	.591	.704	.735		.134	−.126	Pb
Zn	.358	.250	.057	.403	.511	.455	.850	.600	.752	.572	.661	.717		.105	Zn
Ti	.367	.425	−.051	.763	.749	.793	.687	.809	.354	.994	.960	.679	.599		Ti

ACPD
10, 20975–21021, 2010

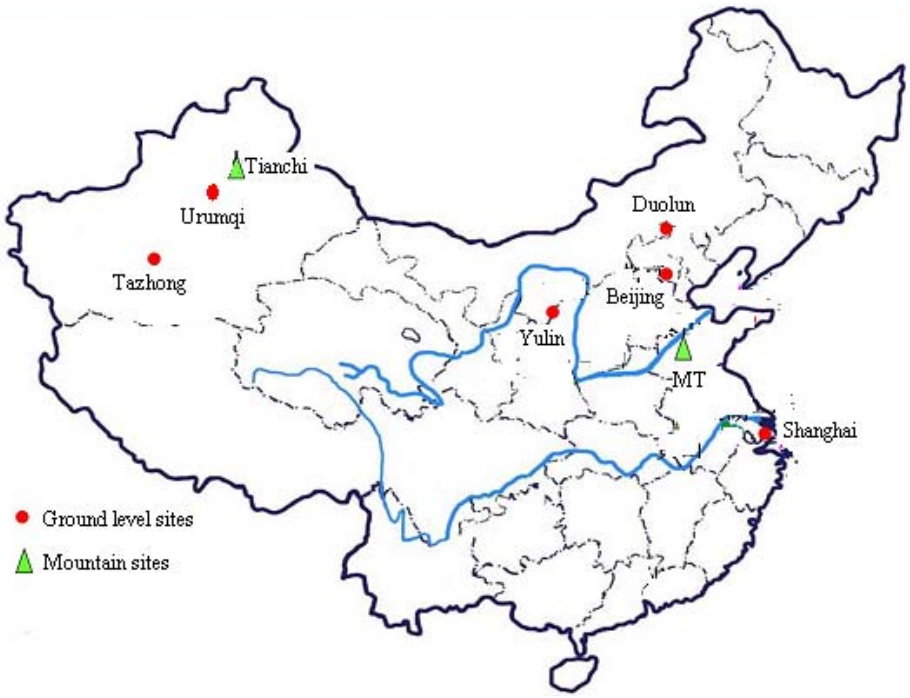

Fig. 1. Map of the sampling sites in this study.

ACPD
10, 20975–21021, 2010

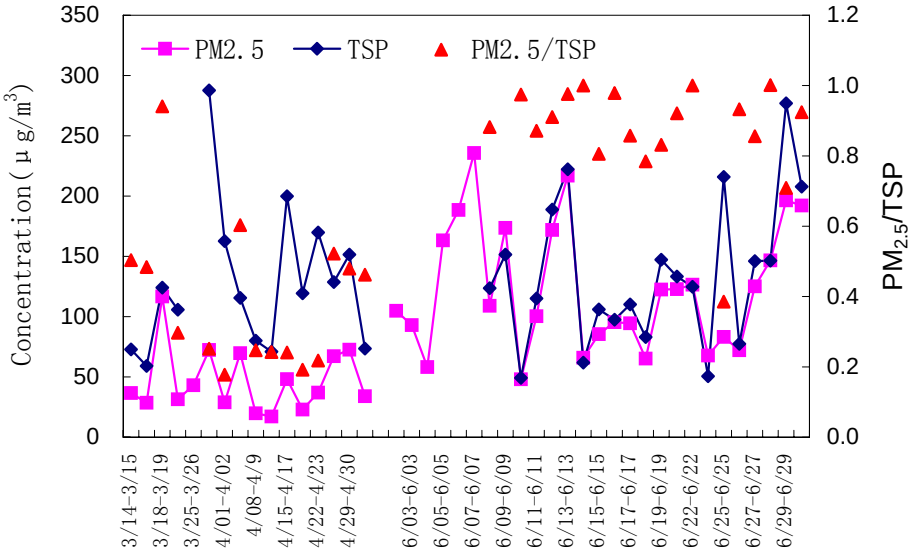

Fig. 2. Daily variations of TSP and $PM_{2.5}$ from 14 March to 29 June in 2006 at MT.

ACPD
10, 20975–21021, 2010

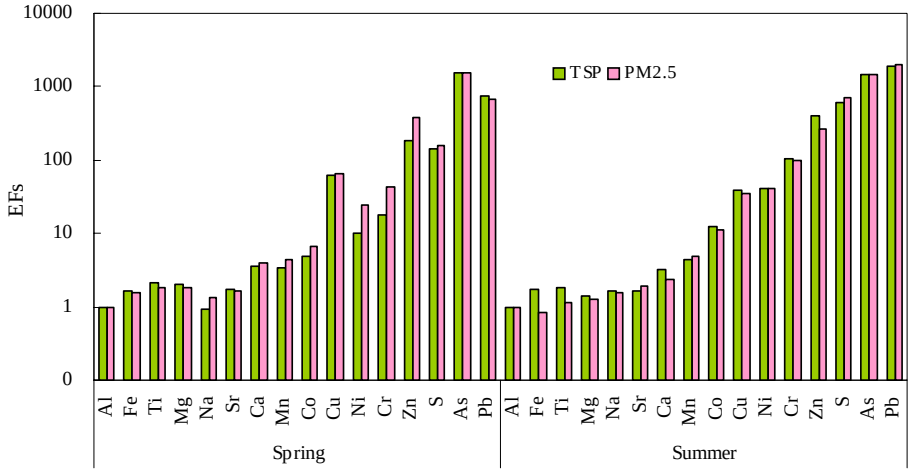

Fig. 3. Enrichment factors (EFs) of elements at MT in spring and summer, 2006.

ACPD
10, 20975–21021, 2010

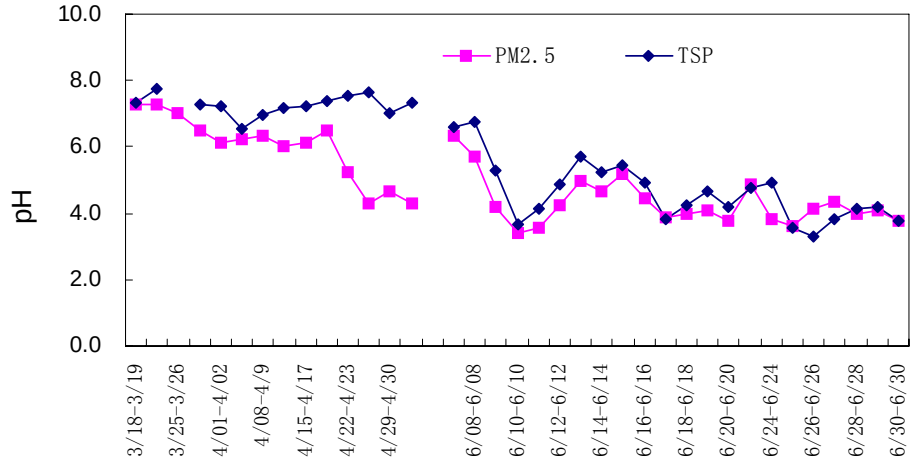

Fig. 4. Daily variations of pH of aqueous filtrates of aerosols at MT, 2006.

ACPD
10, 20975–21021, 2010

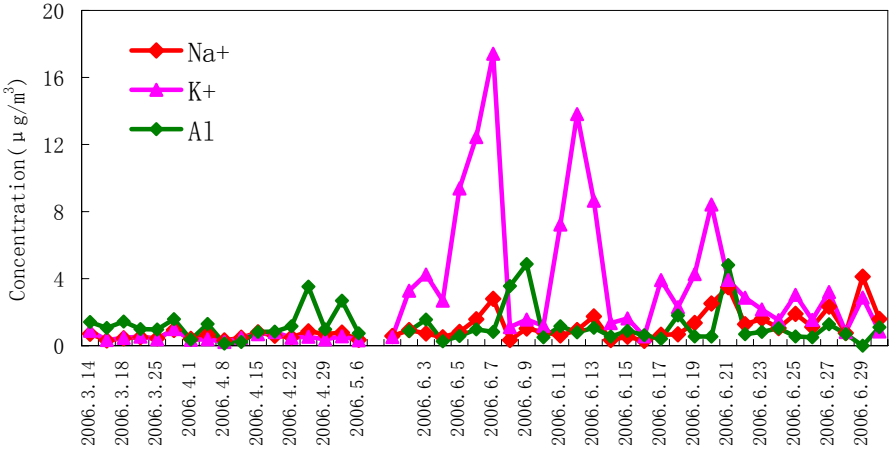

Fig. 5. Daily variations of K^+, Na^+, and Al in $PM_{2.5}$ from March 14 to June 29 in 2006 at MT.

ACPD
10, 20975–21021, 2010

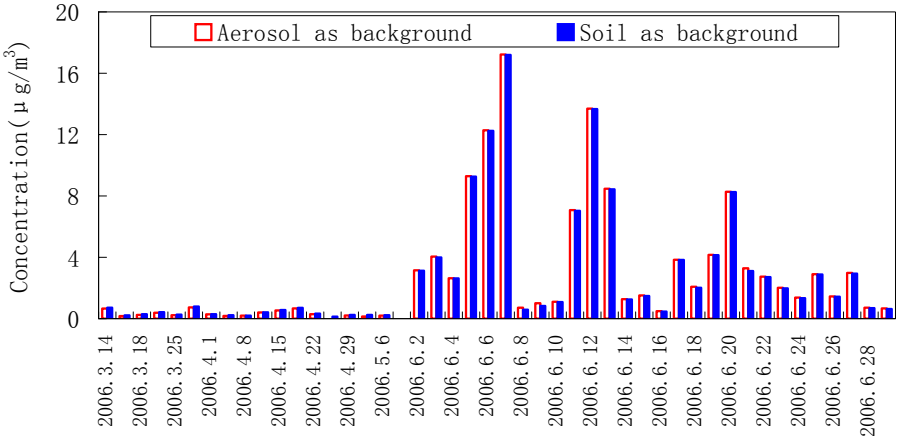

Fig. 6. Water soluble potassium related to biomass burning in $PM_{2.5}$ in 2006 at MT.

ACPD
10, 20975–21021, 2010

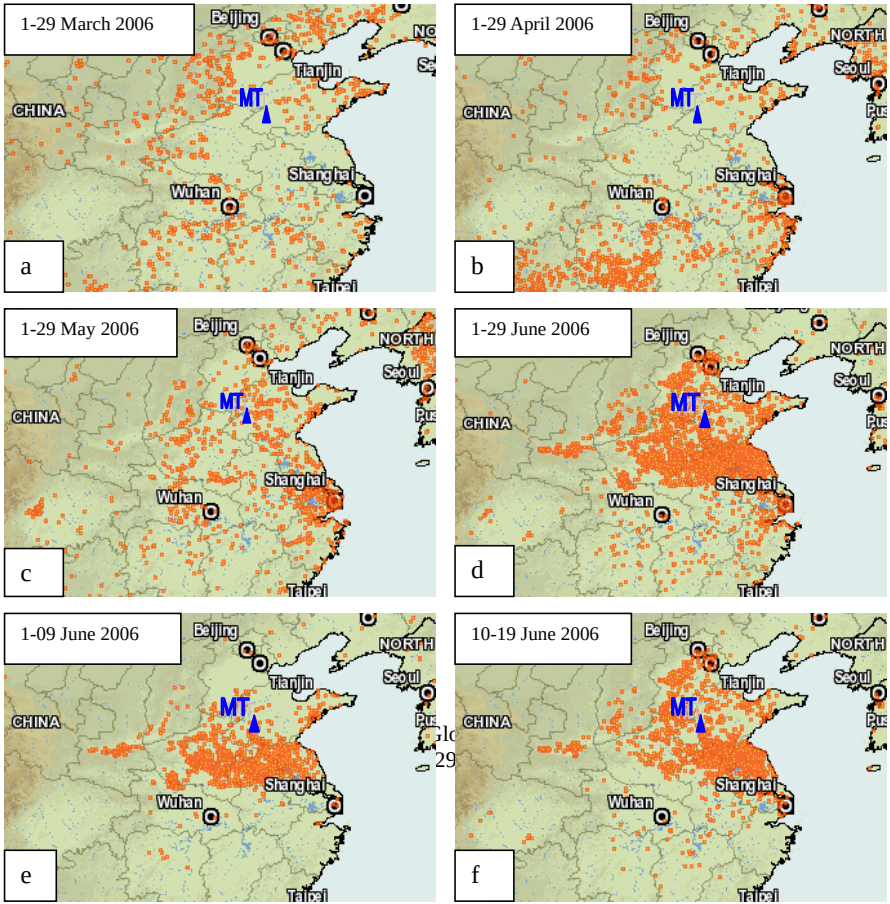

Fig. 7. Fire spot data derived from MODIS Global Fire Mapping during 2006: **(a)** 1–29 March, **(b)** 1–29 April, **(c)** 1–29 May, **(d)** 1–29 June, **(e)** 1–9 June and **(f)** 10–19 June at MT.

ACPD
10, 20975–21021, 2010

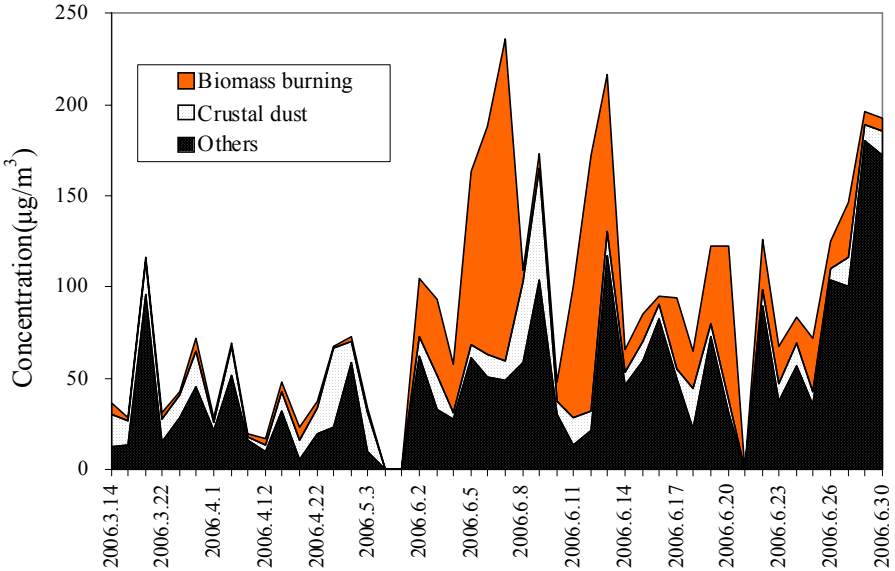

Fig. 8. Temporal compositions of $PM_{2.5}$ from 14 March to 29 June in 2006 at MT.

ACPD
10, 20975–21021, 2010

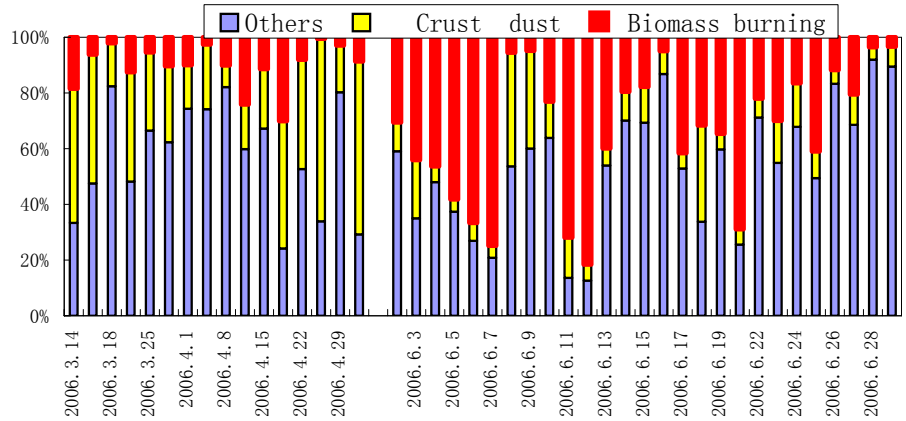

Fig. 9. Distributions of variable source of $PM_{2.5}$ during campaign period at MT.

ACPD
10, 20975–21021, 2010

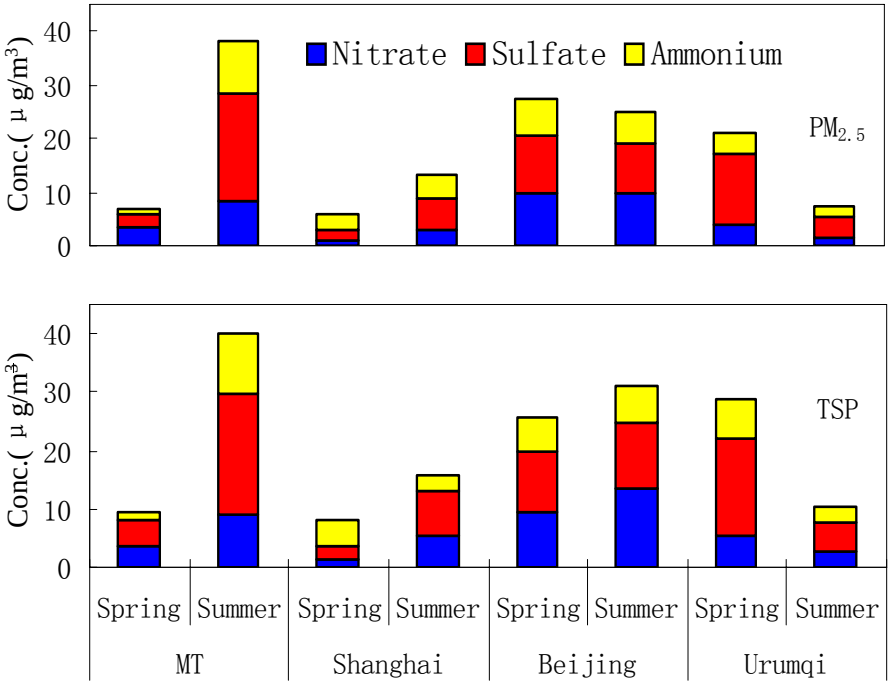

Fig. 10. Seasonal variations of SO_4^{2-}, NO_3^-, and NH_4^+ in aerosols at different sites.

ACPD
10, 20975–21021, 2010

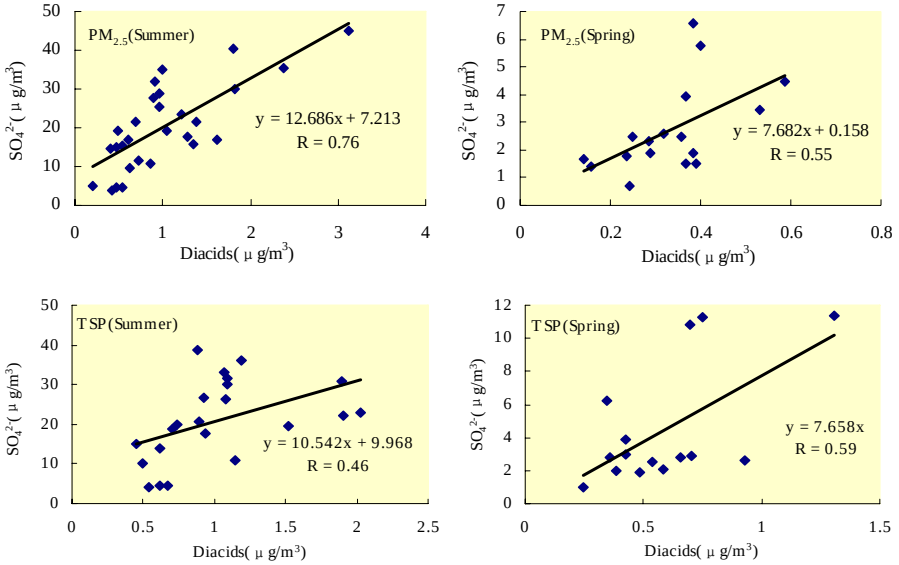

Fig. 11. Scatter plots of SO_4^{2-} vs. diacids (sum of $CH_2C_2O_4^{-2}$, $C_2H_4C_2OO_4^{-2}$, and $C_2O_4^{-2}$).

ACPD
10, 20975–21021, 2010

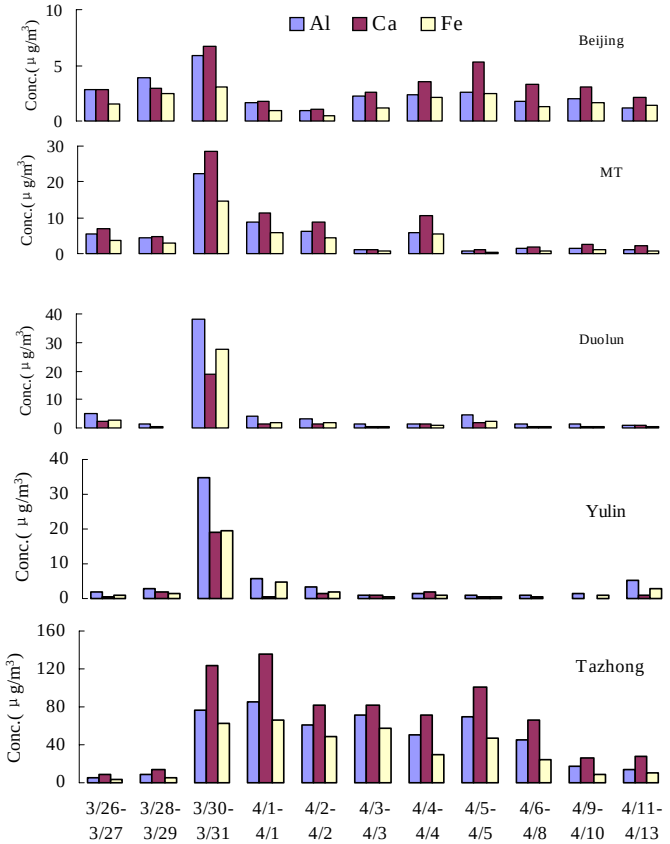

Fig. 12. Daily variation of mineral elements (Ca, Al and Fe) at different sampling sites in spring, 2007.

ACPD
10, 20975–21021, 2010

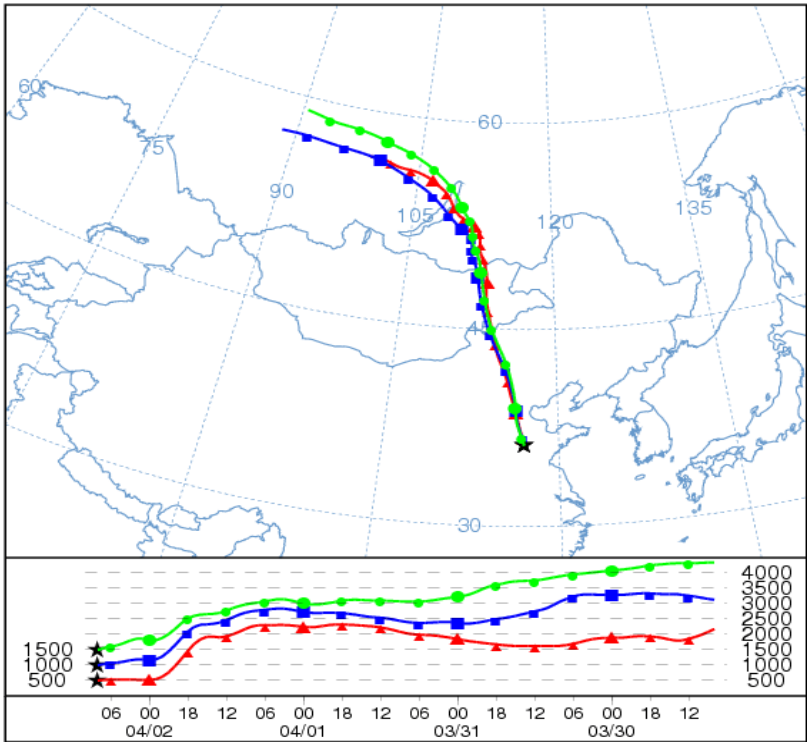

Fig. 13. Back trajectories arriving at MT at 08:00 UTC on 2 April, 2007.

ACPD
10, 20975–21021, 2010

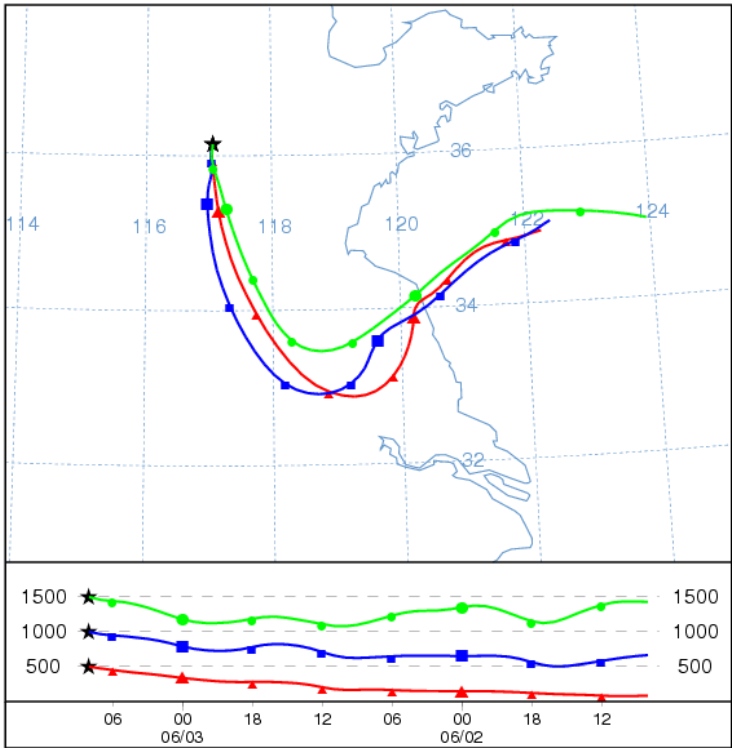

Fig. 14. Back trajectories arriving at MT at 08:00 UTC on 3 June 2006.

ACPD
10, 20975–21021, 2010